Geophysical Research Letters

RESEARCH LETTER
10.1029/2020GL091232

Key Points:

- Quasi-Love waves in the frequency band 7–13 mHz are extracted from the records at stations near the eastern edge of the Ross Sea Embayment (RSE)
- The quasi-Love waves locate an anisotropic boundary in the RSE, which is consistent with a magnetic anomaly boundary
- The vertically coherent boundary in the middle RSE determined by the quasi-Love waves may be caused by vertical mantle flow

Supporting Information:

- Supporting Information S1

Correspondence to:
X. G. Hu,
hxg432@whigg.ac.cn

Citation:
Cheng, W., Hu, X. G., & Liu, L. T. (2021). Anisotropy gradients in the middle of the Ross Sea Embayment, West Antarctica: Evidence from QL scattered surface waves. *Geophysical Research Letters*, *48*, e2020GL091232. https://doi.org/10.1029/2020GL091232

Received 14 OCT 2020
Accepted 22 FEB 2021

Anisotropy Gradients in the Middle of the Ross Sea Embayment, West Antarctica: Evidence From QL Scattered Surface Waves

W. Cheng[1,2], X. G. Hu[1], and L. T. Liu[1]

[1]State Key Laboratory of Geodesy and Earth's Dynamics, Innovation Academy for Precision Measurement Science and Technology, Chinese Academy of Sciences, Wuhan, China, [2]College of Earth and Planetary Sciences, University of Chinese Academy of Sciences, Beijing, China

Abstract Long-period quasi-Love (QL) waves in West Antarctica were detected using the band-pass filtering. Rayleigh waves from March 11, 2011 Tohoku M_w 9.1 earthquake and March 9, 2011 Tohoku M_w 7.3 earthquake had evident QL waves in the frequency range of 7–13 mHz when crossing the Ross Sea Embayment (RSE), while exhibiting normal behavior when crossing the Southern Ocean adjacent to the RSE. We located an anisotropic boundary in the upper mantle beneath the RSE according to the QL waves. Surprisingly, the boundary was consistent with the sharp transition zone of magnetic anomalies discovered by the most recent airborne magnetic surveys. Thus, we speculate that the anisotropic boundary was most likely due to vertical mantle flow below the RSE, which may provide evidence of a vertically coherent boundary condition in the RSE. That anisotropic boundary may be an important tectonic imprint for maintaining the stability of the Ross Ice Shelf.

Plain Language Summary When long-period Love surface waves cross an anisotropic media, they will generate scattered waveforms called quasi-Love waves (QL). QL waves can be used to investigate the mantle anisotropy several hundred kilometers from the stations. QL waves in the narrow frequency band of 7–13 mHz are extracted from the records at stations near the eastern edge of the Ross Sea Embayment (RSE) using a band-pass filter. The QL waves locate a sharp boundary of anisotropic gradient in the upper mantle at depth of 100–200 km beneath the RSE. That boundary divides the RSE into eastern and western RSE. We infer that vertical mantle flow may exist between eastern and western RSE. More attractively, the boundary of mantle anisotropy is consistent with the crustal magnetic anomaly boundary. This linkage suggests a vertically coherent boundary condition through the crust and the upper mantle in the middle RSE. Our observations of QL waves demonstrate the lithosphere beneath the eastern RSE doesn't extend to the foot of the TAM, and we interpret that boundary as the tectonic boundary between West Antarctica and East Antarctica.

1. Introduction

The Ross Sea Embayment (RSE), occupied by the Ross Ice Shelf (RIS), and Ross Sea (RS), comprises the western major sector of the West Antarctic Rift System (WARS). The RSE lies between the Marie Byrd Land Dome (MBL) and the Transantarctic Mountains (TAM), and is surrounded by the TAM in the west and adjacent to the MBL in the east (Figure 1). The bedrock elevations in the MBL are only a few hundred meters, whereas the TAM abruptly uplifts to 4,000 m in the west of the RSE. The dramatic contrasts of bedrock elevations in the MBL and TAM indicate an asymmetric tectonic structure of the RSE (Luyendyk et al., 2003). The notable features of the RSE are low bedrock elevations and a thin crust (<25 km) (Chaput et al., 2014; Wilson & Luyendyk, 2009). The thin crust in the RSE was previously believed to be caused by the large-scale extension of the WARS during the Cretaceous and Cenozoic (Behrendt et al., 1991; Fitzgerald et al., 1986), and the thinned crust in the WARS was generally considered to extend from the western MBL across the RS to the foot of the TAM (e.g., An et al., 2015). However, recent airborne magnetic surveys showed a clear north-south magnetic anomaly boundary in the middle RSE which divides the RSE into two parts with contrasting crustal properties (Tinto et al., 2019), and seismic tomography imaging appears to indicate that the upper mantle structure below the RSE is heterogeneous (e.g., Hansen et al., 2014; Heeszel et al., 2016; Tinto et al., 2019). This evidence of magnetic anomalies and seismic velocity models strongly suggests that

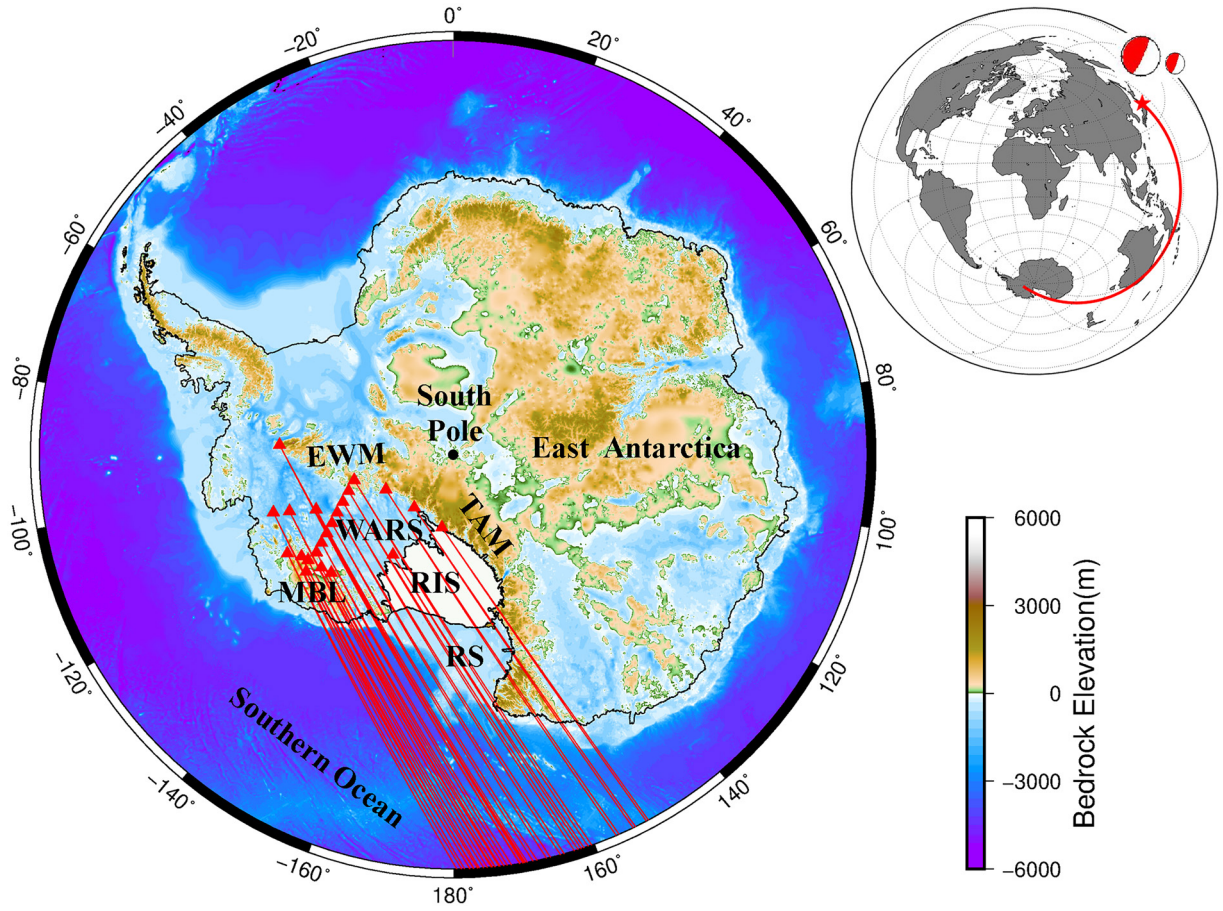

Figure 1. Antarctic stations used in this study and the epicenters of the March 11 (M_w 9.1) and March 9 (M_w 7.3) earthquakes in Tohoku, Japan. The red lines on the Antarctic map with bed elevations (Fretwell et al., 2013) are source-receiver great circle paths for the stations, which just pass through the Ross Sea Embayment (RSE). EWM, Ellsworth-Whitmore Mountains crustal block; MBL, The Marie Byrd Land crustal block; TAM, Transantarctic Mountains; WARS, West Antarctica Rift System; RIS, Ross Ice Shelf; RS, Ross Sea.

the lithosphere in the WARS may not directly extend beneath the RSE to the foot of the TAM. However, to date, there have been no anisotropic surveys of the RSE to confirm the results.

An anisotropic structure can be detected by shear-wave splitting measurements at a seismic station with $a < 50$ km lateral resolution (Savage, 1999). Regional large data sets of anisotropic structures can provide a new constraint on the tectonic history and geodynamics of the upper mantle below the region. However, few anisotropic data sets have been obtained in West Antarctica because of the limited coverage of seismic stations (e.g., Accardo et al., 2014; Barklage et al., 2009; Graw & Hansen, 2017; Hu, 2016; Salimbeni et al., 2010). Seismic stations in West Antarctica are mainly installed at the edges around the RSE and TAM, eastern WARS, and MBL; therefore, no shear-wave splitting measurements have been taken in the majority of WARS, especially in the RSE.

Upon propagation through an anisotropic medium, Love waves are scattered and, thus, generate a Rayleigh-polarized waveform, that is, the quasi-Love (QL) wave. Wave-propagation simulation showed that QL waves are best explained by the presence of lateral gradients of anisotropy along the surface-wave propagation path (Park & Yu, 1993). QL waves observed at certain stations have been used to investigate the azimuthal anisotropy features in plate boundaries in remote subduction zones, which are several hundred kilometers from the stations (e.g., Levin & Park, 1998; Park et al., 2002; Rieger & Park, 2010; Servali et al., 2020; Yu & Park, 1994). Another advantage of the QL wave over shear-wave splitting in the investigation of anisotropy is that the observed QL wave is sensitive to the anisotropy depth, as QL waves are the result of the horizontal integral of anisotropy along the surface-wave propagation paths, whereas shear-wave

splitting measurements are the result of the vertical integral of anisotropy along shear-wave paths (e.g., Long & Silver, 2008). Therefore, observations of QL waves are an important complement to shear-wave splitting measurements in the detection of azimuthal anisotropy. In this study, we investigated QL waves in Rayleigh waves from two earthquakes in Tohoku, Japan at POLENET/ANET seismic network stations in West Antarctica, as their source-receiver propagation paths passed over the RSE and nearby regions (Figure 1). We located the Love-to-Rayleigh scatterers based on the observed delay times between the QL waves and Love waves. The locations of the scatterers form an anisotropic boundary in the central RSE.

2. Data and Observations

2.1. Data and Events

To identify QL wave signals in the observed Rayleigh waves at a station, the source-receiver distance must be >70° (Chen & Park, 2013). QL wave behaviors are similar to those of higher-mode Rayleigh waves; thus, they can be difficult to differentiate (e.g., Kobayashi, 2002). Shallow earthquakes are ideal for observing QL wave because they excite less high-mode Rayleigh waves than deep earthquakes. Generally, QL wave amplitudes recorded on the vertical component of a seismograph are 3%–20% of the amplitudes of the main Love wave on the transverse component (e.g., Yu & Park, 1994), resulting in QL waves being more evident at the Rayleigh-wave radiation minima (e.g., Yu & Park, 1993).

The POLENET/ANET project includes GPS and seismic network that is dedicated to observing the response of the West Antarctic Ice Sheet to a warming global climate. The seismic network part contains a backbone network having more than 20 long-term stations and two seismic arrays located in central West Antarctica. The first array, in which temporary stations are spaced ~90 km apart, extends from MBL to the Ellsworth-Whitmore Mountains, spanning ~1,100 km (Figure 1). A second temporary array with three stations crosses the first array near Mount Sidley. The temporary stations were only operated from January 2010 to January 2012.

We noted that surface waves from two earthquakes, that is, on the March 11, 2011 (M_w 9.1) and March 9, 2011 (M_w 7.3) in Tohoku, Japan, arrived at the stations by propagating through the RSE, and that their small arcs of source-receiver great circle paths were >90°. The March 11 earthquake, with a 24 km focal depth, was the largest earthquake in Japan since 1,900. Its focal mechanism was a reverse fault with an approximately east-west compressional axis. The March 9 earthquake had a fault mechanism and location similar to that of the March 11 earthquake, and was a shallow event with a 20 km depth. The Antarctica stations used in this study were located in weak Rayleigh-wave radiation regions during the two earthquakes, and recorded weak Rayleigh waves but strong Love waves. Therefore, it is possible that QL wave can be more clearly identified in the vertical component of the seismograms of the stations. We obtained low-frequency data (sampling rate of 1 Hz) from the IRIS Data Management Center.

2.2. QL Wave Observations

Anisotropy causes the polarization anomalies of a part of scattered Love waves, producing QL waves in vertical and radial components. QL waves in the radial ground motion component may be contaminated by refracted Love waves, whereas those in the vertical component will not be contaminated; therefore, vertical QL waves can be detected with less ambiguity. The frequency range of QL waves is related to the depth of anisotropy, and the appearance of long-period QL waves indicates an azimuthal anisotropic structure in the upper mantle (Park & Levin, 2002). In this study, we used a band-pass filter to detect QL waves in the vertical component of seismograms at Antarctic stations. QL waves usually exhibit similar characteristics to those of higher-mode Rayleigh waves (Margheriti et al., 2014). To distinguish the ambiguity between QL waves and higher-mode Rayleigh waves, we compared observed Rayleigh waves with predicted waves, which are the synthesis of normal modes computed based on focal mechanisms of earthquakes and spherically isotropic PREM (Dziewonski & Anderson, 1981).

Figure 2 shows a comparison of the observed transverse, vertical and synthetic data from the March 11 earthquake at stations ST14 and SURP. At frequencies <6 mHz, the vertical data are in good agreement with the synthetic data, suggesting that there were no anomalies in the observed Rayleigh waves. In the

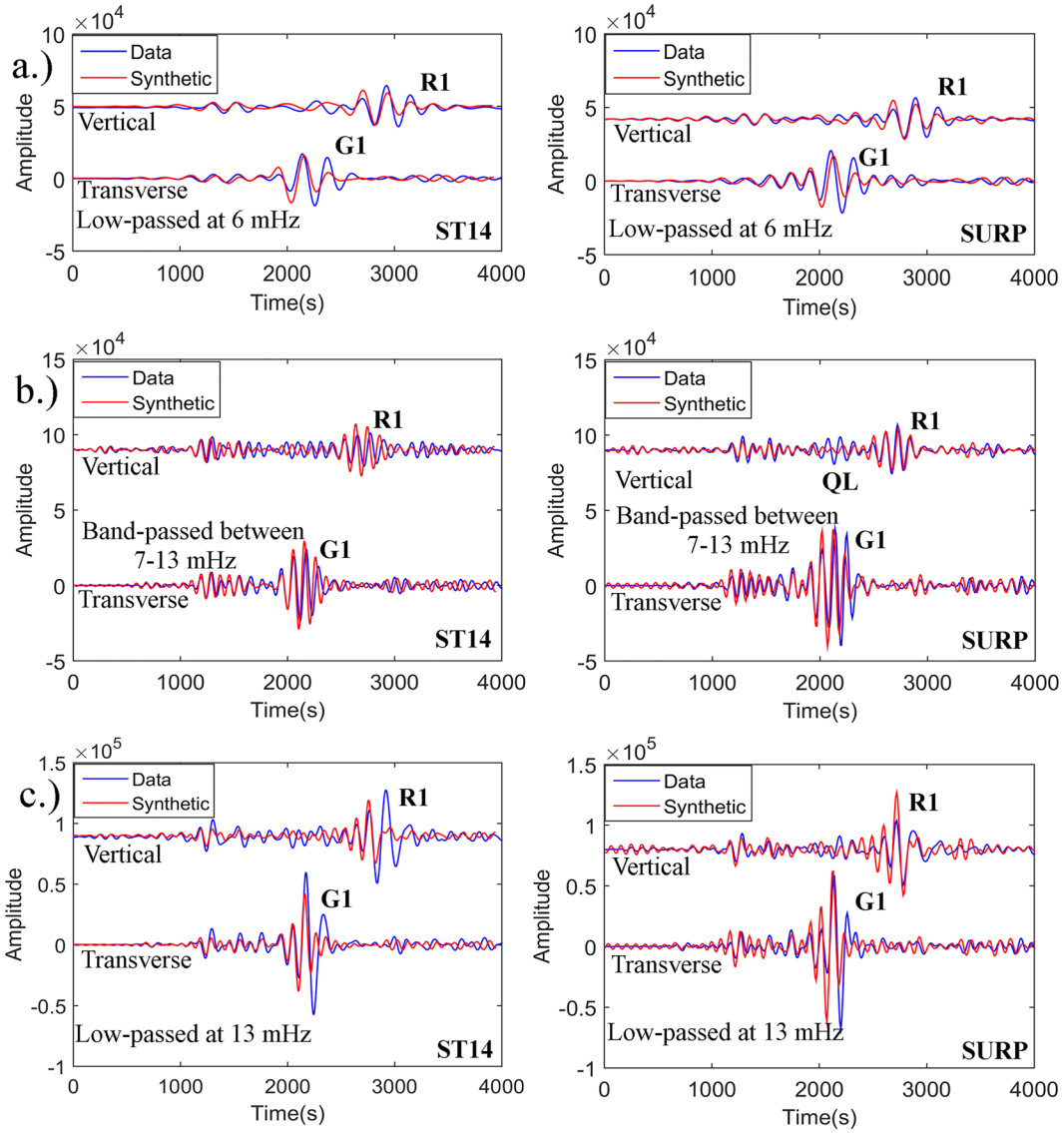

Figure 2. Detected quasi-Love (QL) wave signals by comparison of filtered surface-wave observations and synthetic data from the 11 March earthquake in Tohoku, Japan, at Antarctic stations ST14 and SURP. The synthetic data are summations of normal modes for the isotropic PREM. Both data and synthetics are as follows: (a) Low-pass filtered at 6 mHz; (b) band-pass filtered at 7–13 mHz; and (c) low-pass filtered at 13 mHz. QL wave signals were only obvious in the frequency band of 7–13 mHz at SURP. No QL wave signals were found at ST14.

frequency band of 7–13 mHz, obvious amplitude anomalies occurred in the observed Rayleigh waves at the SURP. The anomalies appeared immediately after the Love wave packet *G*1 but prior to the Rayleigh wave packet *R*1, indicating that they were QL waves (marked as QL in Figure 2). However, there appeared to be no obvious QL waves at ST14 because no similar significant amplitude anomalies occurred between *G*1 and *R*1, although there were Rayleigh wave phase anomalies. Low-pass filters are usually used to detect QL waves (e.g., Park & Yu, 1993), and a small QL wave was observed in seismic records <13 mHz at the SURP station; however, it was inconspicuous compared with that at the frequency band of 7–13 mHz. The QL/Love ratio was 26% at SURP in the 7–13 mHz frequency band and >16% in the low-pass records <13 mHz. The larger QL/Love ratio in the band-pass records suggests that it is more appropriate to use a band-pass filter to extract the QL waves. We attempted to detect QL waves at all 22 stations used in this study (Figures S1 and S2 in the supporting information). QL waves mainly appeared at 12 stations in southern West

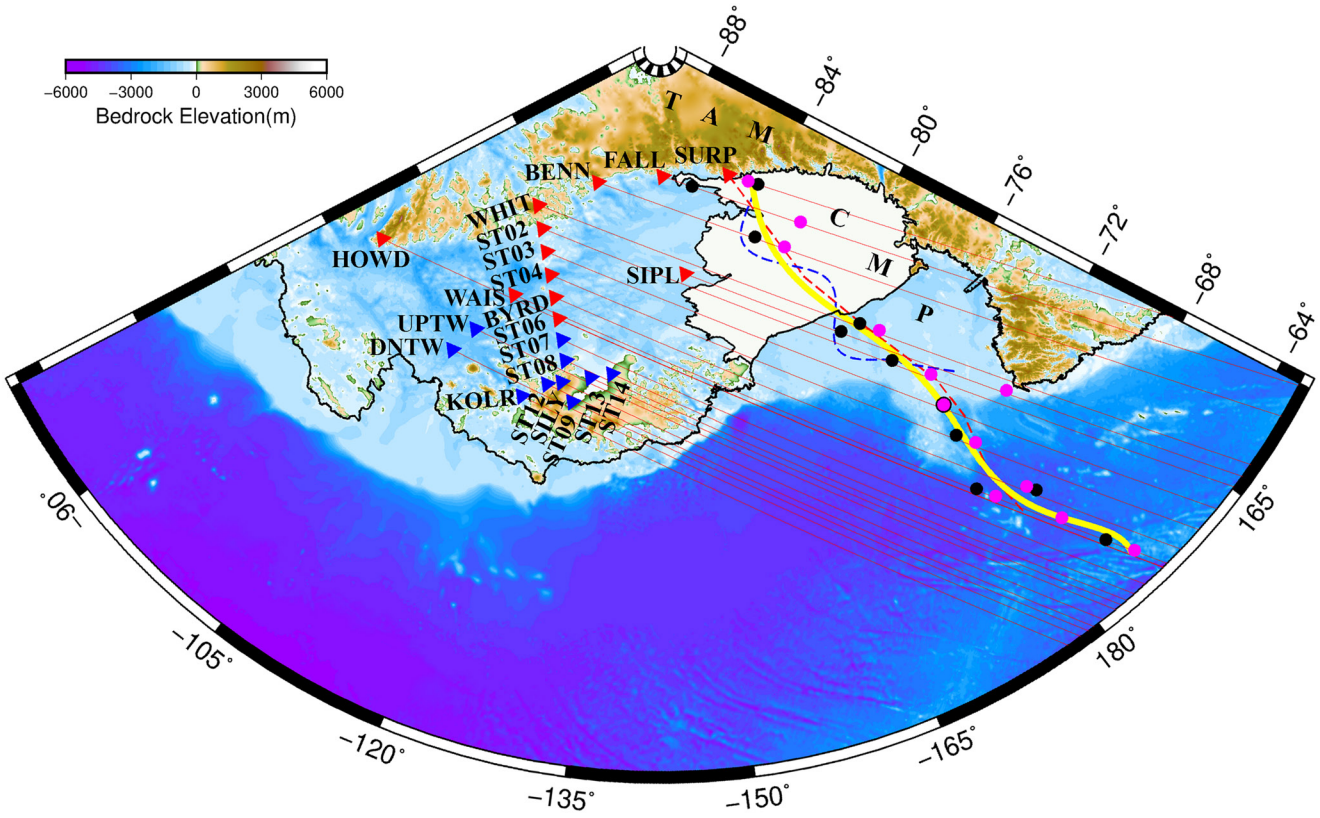

Figure 3. Locations of Love-to-Rayleigh scatterers beneath the RSE inferred by observed QL waves. The stations which recorded obvious QL wave signals are marked by red triangles and others are marked by blue triangles. The scatterer locations inferred by QL waves of the 11 March earthquake in Tohoku, Japan, are marked by black circles and those by QL waves of the 9 March earthquake are marked by magenta circles. The yellow curve is the boundary of anisotropy gradient fitted by the location points, which is close to the magnetic anomaly boundary (dashed red curve) diagnosed by an airborne survey (Tinto et al., 2019) and to the boundary (dashed blue curve) of cooler and warmer mantles at a 200 km depth in the *P*-wave velocity model for the RSE (White-Gaynor et al., 2019). CMP: Cratonic margin province (Jordan et al., 2020).

Antarctica (red triangles in Figure 3), and the six southern stations in the first array recorded obvious QL waves, while other stations in the two arrays did not record QL waves with significant amplitudes.

2.3. Locations of Love-to-Rayleigh Conversion

The anisotropic structure in the upper mantle acts as a surface-wave scatterer, which can convert long-period Love waves into long-period Rayleigh waves (QL waves). The distance between the station and the scatterer can be calculated by the following equation:

$$\delta x = \frac{\delta t}{1/v_R - 1/v_L}, \tag{1}$$

where δt denotes the delay time between the QL waves and Love waves, v_R and v_L denote the phase velocities of the Rayleigh and Love waves, respectively. The accuracy of the Rayleigh and Love wave phase velocities is critical for accurate positioning of the scatterers (Chen & Park, 2013). To improve the reliability of the positioning, we calculated the phase velocities difference of Rayleigh and Love waves at several stations using the two-station method and used the average phase velocity difference to the positioning, the $1/v_R - 1/v_L$ value of 2.59 was used to locate Love-to-Rayleigh conversion scatterers. The time delay between the QL waves and the Love waves was determined using the cross-correlation coefficient method (Table 1; Figure S3 in the supporting information). The distance between the stations and the scatterers was then calculated using Equation 1 and was then back-projected to the source-receiver great circle paths

Table 1
Summary of Quasi-Love (QL) Time Delay at 12 Stations

Stations	Latitude	Longitude	Delay time(s) March 11	Delay time(s) March 9
BENN	−84.573097	−117.392303	16	19
BYRD	−80.016998	−119.473801	50	49
FALL	−85.306602	−143.628403	3	14
SIPL	−81.640503	−148.955307	16	33
ST02	−82.069	−109.124702	36	40
ST03	−81.406502	−113.150803	41	41
ST04	−80.715202	−116.579201	42	44
ST06	−79.331703	−121.820099	55	60
SURP	−84.719902	−171.201706	3	2
WAIS	−79.418098	−111.777901	–	57
WHIT	−82.682297	−104.386703	33	35
HOWD	−77.528603	−86.769402	62	64

(Figure 3). The estimated locations of scatterers formed an approximately north-south boundary in the middle of the RSE.

3. Discussions and Conclusions

As the RSE is covered by the RS and the extremely large RIS, the seismic investigation method has been the main method of understanding the RSE, and currently very little is known about the geology of the RSE due to the harsh Antarctic environment. The RIS is the largest ice shelf in Antarctica, and its stability has drawn much attention in the context of global ocean warming; hence, data and research relevant to Antarctica are valuable. In this study, we fully utilized the limited data regarding West Antarctica. QL waves in the narrow frequency band of 7–13 mHz were extracted from the records at stations near the eastern edge of the RSE using a band-pass filter, as these QL waves are not identified easily using a common low-pass filter. Surface waves from the two earthquakes displayed obvious QL waves at the southern stations in the seismic array; however, no obvious QL waves were observed at the northern stations. Surface waves from two similar co-located events displayed consistent QL wave behavior, suggesting that the observations of QL waves were reliable.

The Love-to-Rayleigh scatterers inferred in this study were clustered around the central line of the RSE and were oriented approximately north-south (Figure 3). These scatterers divided the RSE into two parts: Eastern and western RSE. We plotted the scatterers on the RES map and found that the dividing line was in agreement with the magnetic anomaly boundary discovered by a recent airborne magnetic survey (Tinto et al., 2019). Magnetically, the RSE crust is not homogeneous, and an abrupt boundary in the magnetic anomaly characteristics exists in the middle of the RSE. The eastern RSE crust shows the typical characteristics of high-amplitude magnetic anomalies of the West Antarctica crust; however, the western RSE with low-amplitude magnetic anomalies is similar to that of East Antarctica (Tinto et al., 2019). As the magnetic characteristics of the western RSE are similar to the nearby Neoproterozoic passive margin and subsequent orogenic sediments exposed in the TAM, the western RSE is defined as the "cratonic margin province (CMP)" (Figure 3) (Ferraccioli et al., 2009; Goodge & Finn, 2010; Jordan et al., 2020). The airborne magnetic survey mainly sampled the upper crust, and the lower crust beneath the RSE is also highly heterogeneous according to recent Rayleigh-wave velocity models (Shen et al., 2018) and the 36 s Rayleigh-wave phase velocity map (which samples the lower crust) reveals a clear north-south dichotomy beneath the RSE.

QL waves are sensitive to changes in anisotropy in the Earth's upper mantle (i.e., the gradient of anisotropy) rather than the absolute amount of anisotropy (Chen & Park, 2013). This could be a change in the direction of anisotropy from horizontal to vertical or of rock from isotropic to anisotropic. Simulation experiments have shown that QL waves can be most efficiently generated by the presence of lateral variations of only a few percent (3%–5%) in the azimuthal anisotropy media (HTI anisotropy) rather than lateral heterogeneities, isotropic gradient, or anisotropy with a vertical axis of symmetry (VTI anisotropy) (Park & Yu, 1992; Yu & Park, 1993). However, the VTI anisotropy that is caused by vertical mantle flow can lead to QL waves by inserting new material in a rift, breaking up tectonic regions that either have pre-existing anisotropy with a horizontal (or tilted) symmetry orientation, or developing a horizontal anisotropy orientation during the rifting process.

Long-period QL waves (>70 s) are generally interpreted as evidence of lateral gradients in anisotropy at depths from 100 to 300 km (Maupin & Park, 2007). The dominant period of the QL waves in this study was ~100 s. For the toroidal-spheroidal normal modes coupling near 100 s period, their peak sensitivity kennels were located at a depth of ~150 km, which indicates that the 100 s QL waves have a peak sensitivity near 150 km depth. We infer that the QL waves are caused by the lateral gradients in anisotropy at depths of 100–200 km beneath the middle RSE. The recent high-resolution *P*-wave velocity model within the RSE, which was constructed using data from two dense seismic arrays of the RIS/DRIS network deployed on

the RIS (White-Gaynor et al., 2019), show a clear dichotomy in the upper mantle between the eastern and western basins (Figure 3). As the *P*-wave velocity is sensitive to the mantle temperature, from the *P*-wave velocity structure model, the eastern RSE showed a faster, cooler upper mantle, whereas the slower, warmer mantle characterized the western RSE. In a simple mid-ocean ridge model, the rifting lithosphere shears the underlying mantle in the direction of plate motion, and the LPO of olivine asymptotically aligns with the shear plane. In the LPO of a mid-ocean ridge model, the rotation of the vertical mantle flow directly under the ridge to the horizontal flow away from the ridge could generate a significant lateral gradient in anisotropy (Rieger & Park, 2010). QL waves observed on the west US coast and around Japan have been interpreted as the results of mantle flows in the mid-ocean ridge of the subduction of Cascadia and Japan-Kurile (Kobayashi, 2002; Kobayashi & Nakanish, 1998; Rieger & Park, 2010). A temperature difference of at least ∼100°C occurred in the upper mantle between the eastern and western RSE according to the *P*-wave velocity model (White-Gaynor et al., 2019), indicating that the WARS system underwent multiple phases of rifting processes during the Cretaceous and Cenozoic (Behrendt, 1999; Behrendt et al., 1991). We infer that vertical and horizontal mantle flows may have occurred beneath the central RSE during the large-scale rifting process at the Cretaceous and Cenozoic, that some new materials were inserted into the WARS, and that the lateral gradients in anisotropy may have resulted from the rotation of mantle flow from vertical beneath the central RSE to horizontal away from that middle line.

Observations of QL waves, magnetic anomalies, and high-resolution velocity models jointly proved that there is a clear boundary in the middle of the RSE. These linkages suggest a vertically coherent boundary condition through the crust and upper mantle for the eastern and western RSE. This crust-mantle coupling beneath the middle RSE provides evidence of the dynamic crust-mantle coupling deformation model (Flesch et al., 2005).

The cause of the TAM has been controversial, and different models have been proposed to explain its uplift mechanism, such as the flexure model (Bott & Stern, 1992) and simple shear extension (Fitzgerald et al., 1986). The RSE is adjacent to the TAM, and new understandings of the RSE may help explain the uplift mechanism of the TAM. The abrupt boundary in the middle RSE shows that the eastern RSE does not extend to the foot of the TAM (interpreted as the position of the boundary between West and East Antarctica) rather than the generally accepted prominent TAM (Tinto et al., 2019). The upper mantle surface velocity map and *S*-wave attenuation variations, calculated from the seismic data of regional arrays deployed in the adjacent regions of the RSE and TAM, show that the slower, warmer mantle beneath the CMP extended westward to the crest of the TAM, which may have provided a buoyant thermal load for the asymmetric uplift of the TAM (Lawrence et al., 2006a, 2006b, 2006c).

The magnetic anomaly boundary in the middle RSE was interpreted as a major tectonic boundary between East and West Antarctica, and has an imprint in the bathymetry under the RIS (Tinto et al., 2019). The depth difference of bathymetry beneath the eastern and western RSE plays a positive role in constraining ocean circulation under the RIS and protects the ice shelf ground line from moderate changes in global ocean heat content (Tinto et al., 2019). The QL waves observed in this study indicate that the boundary between the eastern and western RSE is vertically coherent; at the same time, that boundary is a dichotomy line between the cooler and warmer upper mantles in the RSE. As the three boundaries are surprisingly consistent, we infer that the heat flow along that boundary should exhibit a significant change which may influence the stability of the RIS. The boundary of lateral gradients in anisotropy in the upper mantle of the RSE should have a tectonic imprint on the crust above; however, determining its role in the melting of the RIS was beyond the scope of this study. When analyzing the stability of the ice shelf associated with the surface heat flow in the future, this sharp boundary requires further attention.

In this study, the northern stations that recorded surface waves traversing the Southern Ocean (which lies to the north side of the RS) showed no obvious QL waves. Previous studies demonstrated that the amplitude of the QL waves depends on back azimuth (Park, 1997; Rieger & Park, 2010), that the QL wave amplitudes are greatest when the great paths of incoming Love waves align at 45° from the symmetry axis of anisotropy, and that no QL waves are observed when the propagation paths are parallel or perpendicular to the symmetry axis. Therefore, the lack of QL waves at the northern stations of West Antarctica does not rule out lateral gradients in anisotropy; the incoming surface-wave propagation paths may not be suitable for generating clear QL waves. However, the surface waves crossing the RSE presented obvious QL waves, which most

likely indicate the existence of lateral gradients in anisotropy beneath the RSE. The accuracy of locating the Love-to-Rayleigh scatterers mainly depends on the precision of the surface-wave phase velocities, which may have some deviation because of the limited precision of the surface-wave phase velocities in this study; however, most scatterers were clustered near the middle of the RSE.

Data Availability Statement

The data used in this paper were obtained from the IRIS Data Center and are available at: http://ds.iris.edu/mda/YT/?timewindow=2007-2018 (Data ID: https://doi.org/10.7914/SN/YT_2007). GMT software was used to prepare the figures (Wessel & Smith, 2013).

Acknowledgments
The authors thank the reviewers whose constructive comments improved the manuscript. This work was supported by National Natural Science Foundation of China (grants 41674100 and 41374029). The authors would like to thank the IRIS for the seismic data and the mseed2sac software used in this study.

References

Accardo, N. J., Wiens, D. A., Hernandez, S., Aster, R. C., Nyblade, A., Huerta, A., et al. (2014). Upper mantle seismic anisotropy beneath the west Antarctica rift system and surrounding region from shear wave splitting analysis. *Geophysical Journal International*, *198*(1), 414–429. https://doi.org/10.1093/gji/ggu117

An, M. J., Wiens, D. A., Zhao, Y., Feng, M., Nyblade, A. A., Kanao, M., et al. (2015). S-velocity model and inferred Moho topography beneath the Antarctic plate from Rayleigh waves. *Journal of Geophysical Research: Solid Earth*, *120*(1), 359–383. https://doi.org/10.1002/2014JB011332

Barklage, M., Wiens, D. A., Nyblade, A., & Anandakrishnan, S. (2009). Upper mantle seismic anisotropy of south Victoria land and the Ross Sea coast, Antarctica from SKS and SKKS splitting analysis. *Geophysical Journal International*, *178*(2), 729–741. https://doi.org/10.1111/j.1365-246X.2009.04158.x

Behrendt, J. C. (1999). Crustal and lithospheric structure of the west Antarctica rift system from geophysical investigations – A review. *Global and Planetary Change*, *23*(1), 25–44. https://doi.org/10.1016/S0921-8181(99)00049-1

Behrendt, J. C., LeMasurier, W. E., Cooper, A. K., Tessensohn, F., Trehu, A., & Damaske, D. (1991). Geophysical studies of the west Antarctica rift system. *Tectonics*, *10*(6), 1257–1273. https://doi.org/10.1029/91TC00868

Bott, M. H. P., & Stern, T. A. (1992). Finite element analysis of Transantarctic Mountain uplift and coeval subsidence in the Ross Embayment. *Tectonophysics*, *201*(3), 341–356. https://doi.org/10.1016/0040-1951(92)90241-W

Chaput, J., Aster, R. C., Huerta, A., Sun, X., Lloyd, A., Wiens, D., et al (2014). The crustal thickness of West Antarctica. *Journal of Geophysical Research: Solid Earth*, *119*(1), 378–395. https://doi.org/10.1002/2013JB010642

Chen, X. J., & Park, J. (2013). Anisotropy gradients from QL surface waves: Evidence for vertically coherent deformation in the Tibet region. *Tectonophysics*, *608*(26), 346–355. http://dx.doi.org/10.1016/j.tecto.2013.09.019

Dziewonski, A. M., & Anderson, D. L. (1981). Preliminary reference earth model. *Physics of the Earth and Planetary Interiors*, *25*(4), 297–356. https://doi.org/10.1016/0031-9201(81)90046-7

Ferraccioli, F., Armadillo, E., Zunino, A., Bozzo, E., Rocchi, S., & Armienti, P. (2009). Magmatic and tectonic patterns over the Northern Victoria Land sector of the Transantarctic Mountains from new aeromagnetic imaging. *Tectonophysics*, *487*, 43–61. https://doi.org/10.1016/j.tecto.2008.11.028

Fitzgerald, P. G., Sandiford, M., Barrett, P. J., & Gleadow, A. J. W. (1986). Asymmetric extension associated with uplift and subsidence in the Transantarctic Mountains and Ross Embayment. *Earth and Planetary Science Letters*, *81*(1), 67–78. https://doi.org/10.1016/0012-821X(86)90101-9

Flesch, M. L., Holt, W. E., Silver, P. G., Stephenson, M., Wang, C. Y., & Chan, W. W. (2005). Constraining the extent of crust-mantle coupling in central Asia using GPS, geologic, and shear wave splitting data. *Earth and Planetary Science Letters*, *238*(1), 248–268. https://doi.org/10.1016/j.epsl.2005.06.023

Fretwell, P., Pritchard, H. D., Vaughan, D. G., Bamber, J. L., Barrand, N. E., Bell, R., et al. (2013). Bedmap2: Improved ice bed, surface and thickness datasets for Antarctica. *The Cryosphere*, *7*, 371–393.

Goodge, J. W., & Finn, C. A. (2010). Glimpses of East Antarctica: Aeromagnetic and satellite magnetic view from the central Transantarctic Mountains of East Antarctica. *Journal of Geophysical Research*, *115*(B9), B09103. https://doi.org/10.1029/2009JB006890

Graw, J. H., & Hansen, S. E. (2017). Upper mantle seismic anisotropy beneath the Northern Transantarctic Mountains, Antarctica from PKS, SKS, and SKKS splitting analysis. *Geochemistry, Geophysics, Geosystems*, *18*, 544–557. https://doi.org/10.1002/2016GC006729

Hansen, S. E., Graw, J. H., Kenyon, L. M., Nyblade, A. A., Wiens, D. A., Aster, R. C., et al. (2014). Imaging the Antarctica mantle using adaptively parameterized P-wave tomography: Evidence for heterogeneous structure beneath West Antarctica. *Earth and Planetary Science Letters*, *408*(15), 66–78. https://doi.org/10.1016/j.epsl.2014.09.043

Heeszel, D. S., Wiens, D. A., Anandakrishnan, S., Aster, R. C., Dalziel, I. W. D., Huerta, A. D., et al. (2016). Upper mantle structure of central and West Antarctica from array analysis of Rayleigh wave phase velocities. *Journal of Geophysical Research: Solid Earth*, *121*(3), 1758–1775. https://doi.org/10.1002/2015JB012616

Hu, X. G. (2016). Observations of the azimuthal dependence of normal mode coupling below 4 mHz at the South Pole and its nearby stations: Insights into the anisotropy beneath the Transantarctic Mountains. *Physics of the Earth and Planetary Interiors*, *257*, 57–78. https://doi.org/10.1016/j.pepi.2016.05.011

Jordan, T. A., Riley, T. R., & Siddoway, C. S. (2020). The geological history and evolution of West Antarctica. *Nature Reviews Earth & Environment*, *1*(2), 1–17. https://doi.org/10.1038/s43017-019-0013-6

Kobayashi, R. (2002). Polarization anomalies of Love waves observed in and around Japan. *Earth Planets and Space*, *54*, 357–365. https://doi.org/10.1186/BF03352425

Kobayashi, R., & Nakanish, I. (1998). Location of Love-to-Rayleigh conversion due to lateral heterogeneity or azimuthal anisotropy in the upper mantle. *Geophysical Research Letters*, *25*(7), 1067–1070.

Lawrence, J. F., Wiens, D. A., Nyblade, A. A., Anandakrishnan, S., Shore, P. J., & Voigt, D. (2006a). Crust and upper mantle structure of the Transantarctic Mountains and surrounding regions from receiver functions, surface waves, and gravity: Implications for uplift models. *Geochemistry, Geophysics, Geosystems*, *7*(10), Q10011. https://doi.org/10.1029/2006GC001282

Lawrence, J. F., Wiens, D. A., Nyblade, A. A., Anandakrishnan, S., Shore, P. J., & Voigt, D. (2006b). Rayleigh wave phase velocity analysis of the Ross Sea, Transantarctic Mountains, and East Antarctica from a temporary seismograph array. *Journal of Geophysical Research*, *111*(B6), B06302. https://doi.org/10.1029/2005JB003812

Lawrence, J. F., Wiens, D. A., Nyblade, A. A., Anandakrishnan, S., Shore, P. J., & Voigt, D. (2006c). Upper mantle thermal variations beneath the Transantarctic Mountains inferred from teleseismic S-wave attenuation. *Geophysical Research Letters*, *33*(3), L03303. https://doi.org/10.1029/2005GL024516

Levin, V., & Park, J. (1998). Quasi-love phases between Tonga and Hawaii: Observations, simulations and explanations. *Journal of Geophysical Research*, *103*(B10), 24321–24331. https://doi.org/10.1029/98JB02342

Long, M. D., & Silver, P. G. (2008). The subduction zone flow field from seismic anisotropy: A global view. *Science*, *319*(5861), 315–318. https://doi.org/10.1126/science.1150809

Luyendyk, B. P., Wilson, D. S., & Siddoway, C. S. (2003). Eastern margin of the Ross Sea Rift in western Marie Byrd Land, Antarctica: Crustal structure and tectonic development. *Geochemistry, Geophysics, Geosystems*, *4*(10), 1090. https://doi.org/10.1029/2002GC000462

Margheriti, L., Lucente, F. P., Park, J., Pondrelli, S., Levin, V., Steckler, M. S., et al. (2014). Large-scale coherent anisotropy of upper mantle beneath the Italian peninsula comparing quasi-Love waves and SKS splitting. *Journal of Geodynamics*, *82*, 26–38. https://doi.org/10.1016/j.jog.2014.07.007

Maupin, V., & Park, J. (2007). Theory and observations: Wave propagation in anisotropic media. *Treatise on Geophysics*, *1*, 289–321.

Park, J. (1997). Free oscillations in an anisotropic Earth: Path-integral asymptotics. *Geophysical Research Letters*, *129*, 399–411.

Park, J., & Levin, V. (2002). Seismic anisotropy: Tracing plate dynamics in the mantle. *Science*, *296*(5567), 485–489. https://doi.org/10.1126/science.1067319

Park, J., Levin, V., Brandon, M., Lees, J. M., Peyton, V., Gordeev, E. I., et al. (2002). A dangling slab, amplified arc volcanism, mantle flow and seismic anisotropy near the Kamchatka plate corner. *Plate Boundary Zones*, *30*, 295–324. https://doi.org/10.1029/GD030p0295

Park, J., & Yu, Y. (1992). Anisotropy and coupled free oscillations: Simplified models and surface wave observations. *Geophysical Journal International*, *110*(3), 401–420. https://doi.org/10.1111/j.1365-246X.1992.tb02082.x

Park, J., & Yu, Y. (1993). Seismic determination of elastic anisotropy and mantle flow. *Science*, *261*(5125), 1159–1162. https://doi.org/10.1126/science.261.5125.1159

Rieger, D. M., & Park, J. (2010). USArray observations of quasi-Love surface wave scattering: Orienting anisotropy in the Cascadia plate boundary. *Journal of Geophysical Research*, *115*, B05306. https://doi.org/10.1029/2009JB006754

Salimbeni, S., Pondrelli, S., Danesi, S., & Morelli, A. (2010). Seismic anisotropy of the Victoria Land region, Antarctica. *Geophysical Journal International*, *182*(1), 421–432. https://doi.org/10.1111/j.1365-246X.2010.04624.x

Savage, M. K. (1999). Seismic anisotropy and mantle deformation: What have we learned from shear wave splitting? *Reviews of Geophysics*, *37*(1), 65–106.

Servali, A., Long, M. D., Park, J., Benoit, M. H., & Aragon, J. C. (2020). Love-to-Rayleigh scattering across the eastern North American passive margin. *Tectonophysics*, *776*, 228321. https://doi.org/10.1016/j.tecto.2020.228321

Shen, W., Wiens, D. A., Anandakrishnan, S., Aster, R. C., Gerstoft, P., Bromirski, P. D., et al. (2018). The crust and upper mantle structure of central and West Antarctica from Bayesian inversion of Rayleigh wave and receiver functions. *Journal of Geophysical Research: Solid Earth*, *123*(9), 7824–7849. https://doi.org/10.1029/2017JB015346

Tinto, K. J., Padman, L., Siddoway, C. S., Springer, M. R., Fricker, H. A., Das, I., et al. (2019). Ross Ice Shelf response to climate driven by the tectonic imprint on seafloor bathymetry. *Nature Geoscience*, *12*, 441–449. https://doi.org/10.1038/s41561-019-0370-2

Wessel, P., Smith, W. H. F., Scharroo, R., Luis, J., & Wobbe, F. (2013). Generic mapping tools: Improved version released. *Eos*, *94*(45), 409–410. https://doi.org/10.1002/2013EO450001

White-Gaynor, A. L., Nyblade, A. A., Aster, R. C., Wiens, D. A., Bromirski, P. D., Gerstoft, P., et al. (2019). Heterogeneous upper mantle structure beneath the Ross Sea Embayment and Marie Byrd Land, West Antarctica, revealed by P-wave tomography. *Earth and Planetary Science Letters*, *513*, 40–50. https://doi.org/10.1016/j.epsl.2019.02.013

Wilson, D. S., & Luyendyk, B. P. (2009). West Antarctica paleotopography estimated at the Eocene-Oligocene climate transition. *Geophysical Research Letters*, *36*(16), L16302. https://doi.org/10.1029/2009GL039297

Yu, Y., & Park, J. (1993). Upper mantle anisotropy and coupled-mode long-period surface waves. *Geophysical Journal International*, *114*(3), 473–489. https://doi.org/10.1111/j.1365-246X.1993.tb06981.x

Yu, Y., & Park, J. (1994). Hunting for azimuthal anisotropy beneath the Pacific Ocean region. *Journal of Geophysical Research*, *99*(B8), 399–422. https://doi.org/10.1029/94JB00936